frontiers | Frontiers in Physics

TYPE Original Research
PUBLISHED 14 December 2022
DOI 10.3389/fphy.2022.1072746

OPEN ACCESS

EDITED BY
Jordan Yankov Hristov,
University of Chemical Technology and Metallurgy, Bulgaria

REVIEWED BY
Kamal Shah,
University of Malakand, Pakistan
Ndolane Sene,
Cheikh Anta Diop University, Senegal
Kolade Matthew Owolabi,
Federal University of Technology, Nigeria

*CORRESPONDENCE
Omar Abu Arqub,
o.abuarqub@bau.edu.jo

SPECIALTY SECTION
This article was submitted to Statistical and Computational Physics, a section of the journal Frontiers in Physics

RECEIVED 17 October 2022
ACCEPTED 07 November 2022
PUBLISHED 14 December 2022

CITATION
Aal MA, Arqub OA and Maayah B (2022), Hilbert solution, iterative algorithms, convergence theoretical results, and error bound for the fractional Langevin model arising in fluids with Caputo's independent derivative.
Front. Phys. 10:1072746.
doi: 10.3389/fphy.2022.1072746

Hilbert solution, iterative algorithms, convergence theoretical results, and error bound for the fractional Langevin model arising in fluids with Caputo's independent derivative

Mohammad Abdel Aal[1], Omar Abu Arqub[2]* and Banan Maayah[3]

[1]Department of Basic Sciences, Faculty of Arts and Educational Sciences, Middle East University, Amman, Jordan, [2]Department of Mathematics, Faculty of Science, Al Balqa Applied University, Salt, Jordan, [3]Department of Mathematics, Faculty of Science, The University of Jordan, Amman, Jordan

Studying and analyzing the random motion of a particle immersed in a liquid represented in the Langevin fractional model by Caputo's independent derivative is one of the aims of applied physics. In this article, we will attend to a new, accurate, and comprehensive numerical solution to the aforementioned model using the reproducing kernel Hilbert approach. Basically, numerical and exact solutions of the fractional Langevin model are represented using an infinite/finite sum, simultaneously, in the $\Sigma_2(\Xi)$ space. The proof has been sketched for many mathematical theorems such as independence, convergence, error behavior, and completeness of the solution. A sufficient set of tabular results and two-dimensional graphs are shown, and absolute/relative error graphs that express the dynamic behavior of the fractional parameters (α, β) are utilized as well. From an analytical and practical point of view, we noticed that the simulation process and the iterative approach are appropriate, easy, and highly efficient tools for solving the studied model. In conclusion, what we have carried out is presented with a set of recommendations and an outlook on the most important literature used.

KEYWORDS

fractional Langevin model, reproducing kernel Hilbert approach, fractional differential model, Caputo fractional derivative MSC2020, 65L10, fluid dynamics

Abbreviations: FLM, fractional Langevin model; RKHA, reproducing kernel Hilbert approach; FDM, fractional differential model; CFD, Caputo's fractional derivative.

1 Introduction

The Langevin equation, in its fractional issue, is a mathematical dynamic model fundamental in Brownian motion applications to characterize the emergence of physical episodes in oscillating mediums. It is a popularization of the conventional model that utilizes a fractional Gaussian procedure formalized by two vertices, which is much more adaptable to the parameterization of the fractal evolution processes [1–4]. The applications of the FLM can be seen in the stock market, motor control system modeling, photoelectron counting, fluid suspensions, deuteron-cluster dynamics, protein dynamics, evacuation process modeling, financial markets, single-file diffusion, and anomalous transport [5–8]. Commonly, FDMs have wide applications in the formation of many engineering and fluid physics phenomena. In the second half of the last century, the search for more serious numerical algorithms began to control many of the nonlinear problems that appeared with the emergence of fractional derivatives and their emerging applications. However, many studies came into existence, as in the following literature [9–13]. To date, effective analytical and numerical schemes have been developed and successfully applied to deal with different classes of FDMs [14–20].

Although finding accurate solutions to FDMs of different orders in Brownian particle motion placements is an important problem for understanding the dynamic attitudes of oscillatory environments in trifling media, in this article, we contemplate creating an accurate numerical solution to FLMs utilizing the CFD with appropriate boundary data using a new renewal in the RKHA. Here, we will generate effective and straightforward numerical solutions without imposing any restrictions on the nature of the proposed FLM and obtain sufficient convergence while reducing the computation time by exposure to the following model [1–8]:

$$\frac{\partial^{\beta}}{\partial x}\left(\frac{\partial^{\alpha}}{\partial x}+\mu\right)\mathcal{E}(x)=\mathfrak{H}(x,\mathcal{E}(x)), \tag{1}$$

equipped with the posterior boundary condition:

$$\begin{cases}\mathcal{E}(0)-\mathcal{E}_0=0,\\ \dfrac{\partial^{\alpha}}{\partial x}\mathcal{E}(1)-\mathcal{E}_1^{\alpha}=0.\end{cases} \tag{2}$$

Typically, the FDM (Eqs 1, 2) consists of the posterior parameters, functions, and variable effects as attached:

1) $x \in \Xi$: $[0,1]$ stands for the time-coordinate independent domain.
2) $0 \le \alpha, \beta \le 1$ stands for the rank of fractional derivatives applied.
3) $\mathcal{E}$: $[0,1] \to \mathbb{R}$ stands for the particle position.
4) $\frac{\partial^{\gamma}}{\partial x}\mathcal{E}$: $\Xi \to \mathbb{R}$ is the CFD of the rank γ of $\mathcal{E}$ and is given as follows:

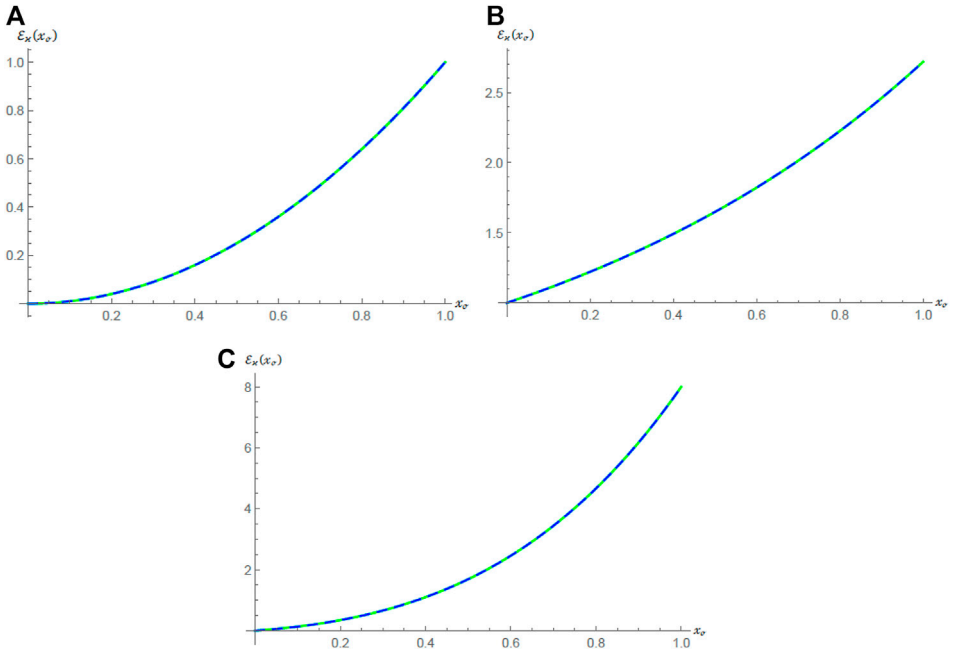

FIGURE 1
2-*D* Cartesian plots of the RKHA numeric solution of the FLM platform over Ξ: **(A)** application 1, when $(\alpha,\beta) = (1/2, 4/5)$; **(B)** application 2, when $(\alpha,\beta) = (1/3, 3/4)$; and **(C)** application 3, when $(\alpha,\beta) = (1/4, 4/5)$.

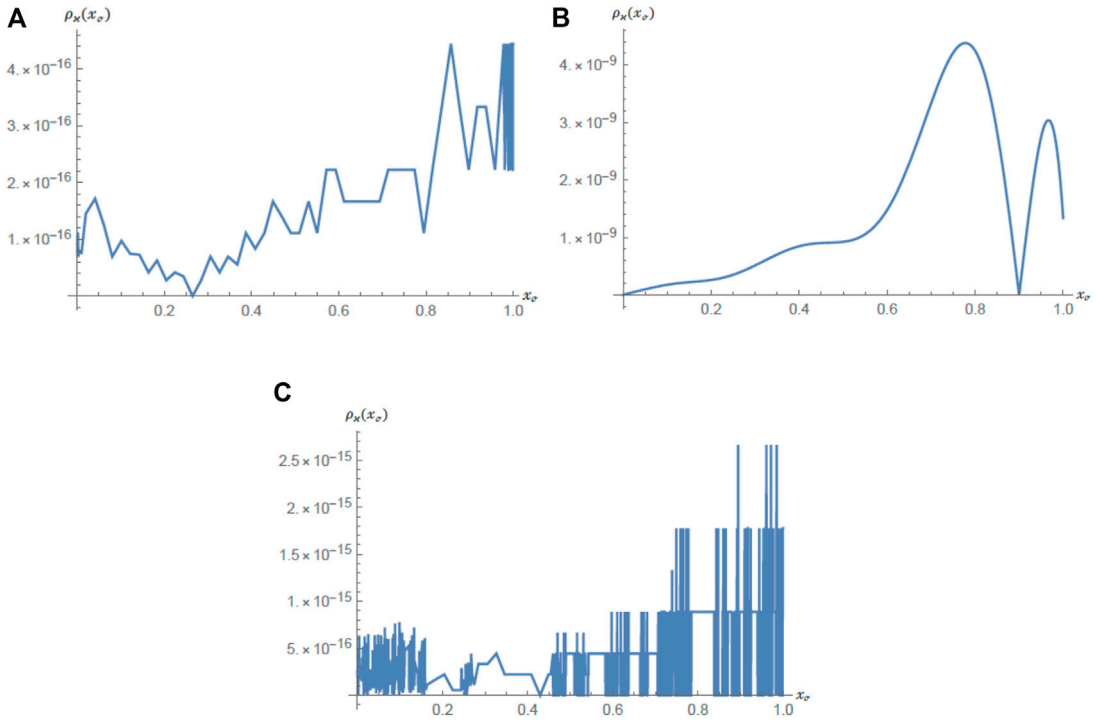

FIGURE 2
2-*D* Cartesian plots of RKHA absolute errors of the FLM platform over Ξ: **(A)** application 1, when $(\alpha, \beta) = (1/2, 4/5)$; **(B)** application 2, when $(\alpha, \beta) = (1/3, 3/4)$; and **(C)** application 3, when $(\alpha, \beta) = (1/4, 4/5)$.

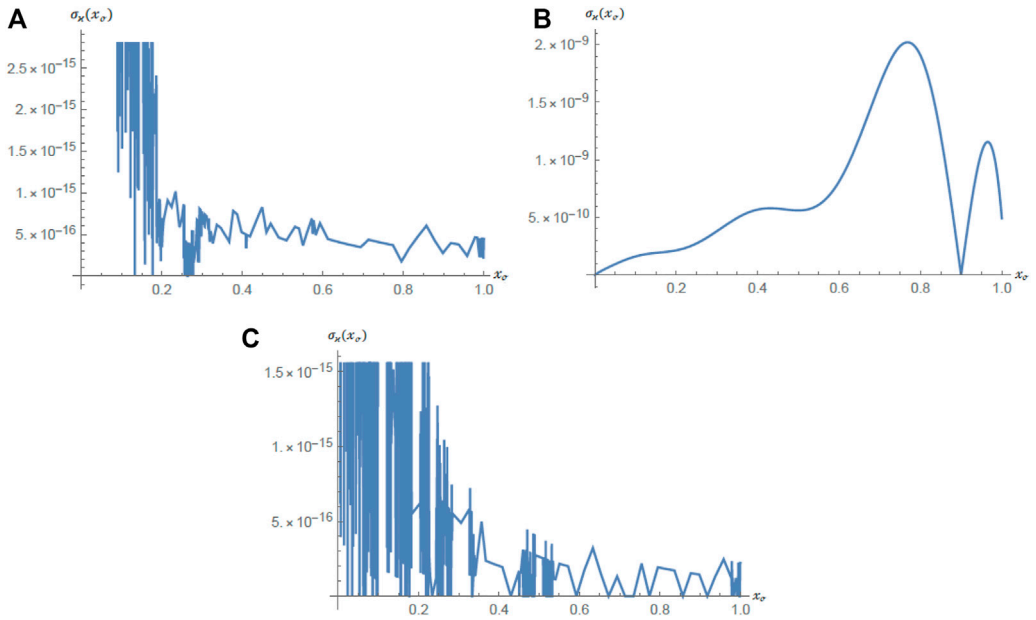

FIGURE 3
2-*D* Cartesian plots of RKHA relative errors of the FLM platform over Ξ: **(A)** application 1, when $(\alpha, \beta) = (1/2, 4/5)$; **(B)** application 2, when $(\alpha, \beta) = (1/3, 3/4)$; and **(C)** application 3, when $(\alpha, \beta) = (1/4, 4/5)$.

TABLE 1 Associated RKHA scores for application 1 with $\varkappa = 101$, when $(\alpha, \beta) = (1/2, 4/5)$.

x_o	$\mathcal{E}(x_o)$	$\mathcal{E}_\varkappa(x_o)$	$\rho_\varkappa(x_o)$	$\sigma_\varkappa(x_o)$
0	0	0	0	∞
0.1	0.01	0.01000000000000009	$9.194034423 \times 10^{-17}$	$9.194034423 \times 10^{-15}$
0.2	0.04	0.03999999999999999	$2.081668171 \times 10^{-17}$	$5.204170428 \times 10^{-16}$
0.3	0.09	0.08999999999999998	$4.163336342 \times 10^{-17}$	$4.625929269 \times 10^{-16}$
0.4	0.16	0.15999999999999992	$1.110223025 \times 10^{-16}$	$6.938893904 \times 10^{-16}$
0.5	0.25	0.24999999999999990	$1.110223025 \times 10^{-16}$	$4.440892099 \times 10^{-16}$
0.6	0.36	0.35999999999999993	$1.665334537 \times 10^{-16}$	$4.625929269 \times 10^{-16}$
0.7	0.49	0.48999999999999990	$2.220446049 \times 10^{-16}$	$4.531522549 \times 10^{-16}$
0.8	0.64	0.63999999999999980	$3.330669074 \times 10^{-16}$	$5.204170428 \times 10^{-16}$
0.9	0.81	0.80999999999999960	$4.440892099 \times 10^{-16}$	$5.482582838 \times 10^{-16}$
1	1	0.99999999999999980	$2.220446049 \times 10^{-16}$	$2.220446049 \times 10^{-16}$

TABLE 2 Associated RKHA scores for application 2 with $\varkappa = 101$, when $(\alpha, \beta) = (1/3, 3/4)$.

x_o	$\mathcal{E}(x_o)$	$\mathcal{E}_\varkappa(x_o)$	$\rho_\varkappa(x_o)$	$\sigma_\varkappa(x_o)$
0	1	1	0	$2.220446049 \times 10^{-16}$
0.1	1.1051709180756477	1.1051709182537852	$1.781375047 \times 10^{-10}$	$1.611854799 \times 10^{-10}$
0.2	1.2214027581601699	1.2214027584214940	$2.613240735 \times 10^{-10}$	$2.139540555 \times 10^{-10}$
0.3	1.3498588075760032	1.3498588080897970	$5.137938963 \times 10^{-10}$	$3.806278801 \times 10^{-10}$
0.4	1.4918246976412703	1.4918246984882728	$8.470024682 \times 10^{-10}$	$5.677627335 \times 10^{-10}$
0.5	1.6487212707001282	1.6487212716247421	$9.246139410 \times 10^{-10}$	$5.608067036 \times 10^{-10}$
0.6	1.8221188003905090	1.8221188018679133	$1.477404199 \times 10^{-9}$	$8.108166156 \times 10^{-10}$
0.7	2.0137527074704766	2.0137527108024590	$3.331982246 \times 10^{-9}$	$1.6546134160 \times 10^{-9}$
0.8	2.2255409284924680	2.2255409327352247	$4.242756813 \times 10^{-9}$	$1.9063935240 \times 10^{-9}$
0.9	2.4596031111569500	2.4596031111516954	$5.254463531 \times 10^{-12}$	$2.136305450 \times 10^{-12}$
1	2.7182818284590450	2.7182818271214640	$1.337581157 \times 10^{-9}$	$4.920686085 \times 10^{-10}$

$$\frac{\partial^{\gamma}}{\partial x}\mathcal{E}(x) = \begin{cases} \dfrac{1}{\Gamma(1-\gamma)}\displaystyle\int_0^x (x-\omega)^{-\gamma}\frac{\partial}{\partial x}\mathcal{E}(\omega)d\omega, & 0<\gamma<1, \\ \dfrac{\partial}{\partial x}\mathcal{E}(x), & \gamma = 1. \end{cases} \tag{3}$$

6) $\mathfrak{H}$: $\Xi \times \mathbb{R} \to \mathbb{R}$ is a bounded variational map that symbolizes the imposed acting on Brownian particles.
7) $\mu \in \mathbb{R}$ is a nontrivial parameter that represents the damping or viscosity term.
8) $\mathcal{E}_0, \mathcal{E}_1^{\alpha} \in \mathbb{R}$ are nontrivial parameters that represent the initial and terminal positions of the particle simultaneously.

Ordinarily, no conventional schemes produce an accurate prototype solution for FLMs. Thus, there is a great need for the RKHA, which satisfies the purpose, as usual, and has reached the desired and satisfactory numerical results with fully stochastic properties. Here, the relevant theories and facts have been confirmed by numeric emulations, graphical representation, and scale tables for three types of FLMs. However, the tenor of the paper is arranged as follows: Section 1: Presentation: FDMs and CFDs. Section 2: RKHA: Preliminaries and definitions. Section 3: RKHA: Construction and properties. Section 4: RKHA: Solutions and convergence. Section 5: Error: Estimation and bound. Section 6: Justifications: Algorithms,

TABLE 3 Associated RKHA scores for application 3 with $\varkappa = 101$, when $(\alpha, \beta) = (1/4, 4/5)$.

x_σ	$\mathcal{E}(x_\sigma)$	$\mathcal{E}_\varkappa(x_\sigma)$	$\rho_\varkappa(x_\sigma)$	$\sigma_\varkappa(x_\sigma)$
0	0	0	0	∞
0.1	0.1331000000000000	0.1331000000000007	$6.938893904 \times 10^{-16}$	$5.213293692 \times 10^{-15}$
0.2	0.3456000000000001	0.3456000000000002	$1.110223025 \times 10^{-16}$	$3.212450881 \times 10^{-16}$
0.3	0.6591000000000001	0.6591000000000005	$3.330669074 \times 10^{-16}$	$5.053359238 \times 10^{-16}$
0.4	1.0976000000000001	1.0976000000000006	$4.440892099 \times 10^{-16}$	$4.046002276 \times 10^{-16}$
0.5	1.6875000000000000	1.6875000000000002	$2.220446049 \times 10^{-16}$	$1.315819881 \times 10^{-16}$
0.6	2.4576000000000007	2.4576000000000010	$4.440892099 \times 10^{-16}$	$1.807003621 \times 10^{-16}$
0.7	3.4391000000000007	3.4391000000000010	$4.440892099 \times 10^{-16}$	$1.291294844 \times 10^{-16}$
0.8	4.6656000000000010	4.6656000000000010	0	0
0.9	6.1731000000000010	6.1731000000000000	$8.881784197 \times 10^{-16}$	$1.438788323 \times 10^{-16}$
1	8.0000000000000000	8.0000000000000000	0	0

applications, and analyses. Section 7: Outline: Conclusion and outlook.

2 Reproducing kernel: Preliminaries and definitions

The approach of the reproducing kernel is a novel solver built to find solutions to FDMs emerging in physics, waves, statistics, and engineering [21–23]. This technique is based on the Gram–Schmidt process and Fourier expansion approach for an arbitrary order and is used for optimizing an orthogonal basis to detect unknown compounds. The RKHA has many motivational aspects and a great ability to handle complicated problems without imposing any restrictions on the style of the models. Therefore, it has been gaining a lot of solicitude and examination lately [24–32].

First, a reproducing kernel induced from a given Hilbert space is called the RKHA. Here, $|\mathfrak{C}|(\Xi)$ is a set of maps that are continuous absolutely on Ξ. At the outset, some requirements that are necessary to go further in our RKHA scheme will be sought.

Remark 1. [24] The frameworks of $\Sigma_0(\Xi)$ are as follows:

$$\begin{cases} \Sigma_0(\Xi) = \{\mathcal{E}\colon \mathcal{E} \in |\mathfrak{C}|(\Xi) \wedge \mathcal{E} \in L^2(\Xi)\}, \\ \langle \mathcal{E}_1(x), \mathcal{E}_2(x)\rangle_{\Sigma_0} = \mathcal{E}_1(0)\mathcal{E}_2(0) + \int_\Xi \mathcal{E}_1'(x)\mathcal{E}_2'(x)dx, \\ \|\mathcal{E}\|^2_{\Sigma_0} = \langle \mathcal{E}(x), \mathcal{E}(x)\rangle_{\Sigma_0}, \\ \Pi_x^{\{1\}}(\jmath) = 1 + \begin{cases} \jmath, & \jmath \le x, \\ x, & \jmath > x. \end{cases} \end{cases} \tag{4}$$

Remark 2. [24] The frameworks of $\Sigma_1(\Xi)$ are as follows:

$$\begin{cases} \Sigma_1(\Xi) = \left\{\mathcal{E}\colon \mathcal{E}^{(\sigma)} \in |\mathfrak{C}|(\Xi) \wedge \mathcal{E}^{(\sigma)} \in L^2(\Xi) \wedge \mathcal{E}(0) = 0\right\}, \\ \langle \mathcal{E}_1(x), \mathcal{E}_2(x)\rangle_{\Sigma_1} = \sum_{\sigma=0}^{1} \mathcal{E}_1^{(\sigma)}(0)\mathcal{E}_2^{(\sigma)}(0) + \mathcal{E}_1(1)\mathcal{E}_2(1) \\ \qquad\qquad + \int_\Xi \mathcal{E}_1'''(x)\mathcal{E}_2'''(x)dx, \\ \|\mathcal{E}\|^2_{\Sigma_1} = \langle \mathcal{E}(x), \mathcal{E}(x)\rangle_{\Sigma_1}, \\ \Pi_x^{\{1\}}(\jmath) = \dfrac{1}{120} \begin{cases} \Pi(\jmath, x), & \jmath \le x, \\ \Pi(x, \jmath), & \jmath > x, \end{cases} \end{cases} \tag{5}$$

with $\Pi(\jmath, x) = \jmath(-120(-1+x)x - x(120 - 246x + 10x^2 - 5x^3 + x^4)\jmath + 5(-1+x)x\jmath^3 - (-1+x^2)\jmath^4)$.

Definition 1 The framework of $\Sigma_2(\Xi)$ is as follows:

$$\Sigma_2(\Xi) = \left\{\mathcal{E}\colon \mathcal{E} \in \Sigma_1(\Xi) \wedge \frac{\partial^\alpha}{\partial x}\mathcal{E}(1) = 0\right\}. \tag{6}$$

Here, one can find that $\Sigma_2(\Xi)$ is a subset in $\Sigma_1(\Xi)$ and is closed. Next, to generate the kernel function of $\Sigma_2(\Xi)$, we put $\Lambda\mathcal{E}(x) = /\mathcal{E}(x)|_{x=1}$.

Theorem 1. If $\Lambda_x\Lambda_\jmath\Pi_x^{\{1\}}(\jmath) \neq 0$, then the framework function of $\Sigma_2(\Xi)$ is as follows:

$$\left\{\Pi_x^{\{2\}}(\jmath) = \Pi_x^{\{1\}}(\jmath) - \frac{\Lambda_x\Pi_x^{\{1\}}(\jmath)\Lambda_\jmath\Pi_x^{\{1\}}(\jmath)}{\Lambda_x\Lambda_\jmath\Pi_x^{\{1\}}(\jmath)}. \right. \tag{7}$$

Proof: Because $\partial^\alpha/\partial\jmath\Pi_1^{\{2\}}(x) = 0$, $\Pi_x^{\{2\}}(\jmath) \in \Sigma_2(\Xi)$. However, for each $\mathcal{E}(\jmath)$ in $\Sigma_2(\Xi)$, one can obtain

$$\begin{aligned} \langle \mathcal{E}(\jmath), \Pi_x^{\{2\}}(\jmath)\rangle &= \langle \mathcal{E}(\jmath), \Pi_x^{\{1\}}(\jmath)\rangle \\ &= \mathcal{E}(x), \end{aligned} \tag{8}$$

or $\Pi_x^{\{2\}}(\jmath)$ is the reproducing kernel of $\Sigma_2(\Xi)$.

Theorem 2. If $\mathcal{E} \in \Sigma_2(\Xi)$, then $|\mathcal{E}(x)| \le 3.5\|\mathcal{E}\|_{\Sigma_2}$, $|\mathcal{E}'(x)| \le 3\|\mathcal{E}\|_{\Sigma_2}$, and $|\mathcal{E}''(x)| \le 2\|\mathcal{E}\|_{\Sigma_2}$.

Proof: Since $\mathcal{E}, \mathcal{E}', \mathcal{E}'', \mathcal{E}''' \in |\mathfrak{C}|(\Xi)$, applying successive integration from 0 to x for $\mathcal{E}'''$, $\mathcal{E}''$, and $\mathcal{E}'$, one can obtain

$$\mathcal{E}''(x) - \mathcal{E}''(0) = \int_0^x \mathcal{E}'''(p)dp, \tag{9}$$

$$\mathcal{E}'(x) - \mathcal{E}'(0) - \mathcal{E}''(0)x = \int_0^x \left(\int_0^{x_1} \mathcal{E}'''(p)dp \right) dx_1, \tag{10}$$

$$\mathcal{E}(x) - \mathcal{E}(0) - \mathcal{E}'(0)x - 0.5\mathcal{E}''(0)x^2 = \int_0^x \left(\int_0^{x_2} \left(\int_0^{x_1} \mathcal{E}'''(p)dp \right) dx_1 \right) dx_2. \tag{11}$$

Taking $|\cdot|$ values and using the fact $0 \le |x|, |x|^2 \le 1$, we can obtain

$$|\mathcal{E}(x)| \le |\mathcal{E}(0)| + |\mathcal{E}'(0)| + 0.5|\mathcal{E}''(0)| + \int_\Xi |\mathcal{E}'''(p)|dp. \tag{12}$$

To complete, one can get $|\mathcal{E}(0)| = \sqrt{\mathcal{E}^2(0)} \le \|\mathcal{E}\|_{\Sigma_2}$, $|\mathcal{E}'(0)| = \sqrt{(\mathcal{E}'(0))^2} \le \|\mathcal{E}\|_{\Sigma_2}$, $|\mathcal{E}''(0)| = \sqrt{(\mathcal{E}''(0))^2} \le \|\mathcal{E}\|_{\Sigma_2}$, and $\int_\Xi [zwj]|\mathcal{E}'''(x)|dx \le \sqrt{\int_\Xi [zwj](\mathcal{E}'''(x))^2 dx} \le \|\mathcal{E}\|_{\Sigma_2}$.

3 Reproducing kernel: Construction and properties

Herein, the boundaries in Eq. 2 will first be homogenized to zero to obtain easy-to-access modeling in the proposed $\Sigma_2(\Xi)$ space. The form of the operator that formulates the required solution will also be determined in addition to some of what is needed for the scheme.

To achieve this, one must first carry out the following:

$$\frac{\partial^\beta}{\partial x}\left(\frac{\partial^\alpha}{\partial x} + \mu\right)\mathcal{E}(x) = \bar{\mathfrak{H}}(x, \mathcal{E}(x)), \tag{13}$$

equipped with the posterior boundary condition:

$$\begin{cases} \mathcal{E}(0) = 0, \\ \dfrac{\partial^\alpha}{\partial x}\mathcal{E}(1) = 0. \end{cases} \tag{14}$$

For the briefing, the normalizing modified version in Eqs 13, 14 was obtained from the posterior underlying conversion, taking into account that all the extra terms transformed into $\bar{\mathfrak{H}}(x, \mathcal{E}(x))$ as

$$\mathcal{E}(x): \ \to \mathcal{E}(x) - (0.5\Gamma(3-\alpha)\mathcal{E}_1^\alpha x^2 + \mathcal{E}_0), \tag{15}$$

$$\bar{\mathfrak{H}}(x, \mathcal{E}(x)) \coloneqq \left(\frac{\Gamma(3-\alpha)}{\Gamma(3-\alpha-\beta)} + \mu\frac{\Gamma(3-\alpha)}{\Gamma(3-\beta)}x^\alpha \right)\mathcal{E}_1^\alpha x^{2-\alpha-\beta} + \mathfrak{H}(x, \mathcal{E}(x) - 0.5\Gamma(3-\alpha)\mathcal{E}_1^\alpha x^2 - \mathcal{E}_0). \tag{16}$$

The conversions in Eqs 15, 16 are needful to insert the equipped boundaries in Eq. 2 inside $\Sigma_2(\Xi)$. Indeed, we will denote $\mathcal{E}$ to new and old solutions always.

1) Define the map $\mathfrak{d}$ such that

$$\mathfrak{d}: \Sigma_2(\Xi) \to \Sigma_0(\Xi). \tag{17}$$

2) Build the $\mathfrak{d}[\mathcal{E}]$ operator as

$$\mathfrak{d}[\mathcal{E}](x) \coloneqq \frac{\partial^\beta}{\partial x}\left(\frac{\partial^\alpha}{\partial x} + \mu\right)\mathcal{E}(x). \tag{18}$$

3) Reframe the FLM problem to solve such that

$$\begin{cases} \mathfrak{d}[\mathcal{E}](x) \coloneqq \bar{\mathfrak{H}}(x, \mathcal{E}(x)), \\ \mathcal{E}(0) = 0, \\ \dfrac{\partial^\alpha}{\partial x}\mathcal{E}(1) = 0. \end{cases} \tag{19}$$

Theorem 3. $\mathfrak{d}: \Sigma_2(\Xi) \to \Sigma_0(\Xi)$ is a bounded linear operator.

Proof: From Remark 1, one can obtain

$$\|\mathfrak{d}\mathcal{E}(x)\|_{\Sigma_0}^2 = \langle \mathfrak{d}\mathcal{E}(x), \mathfrak{d}\mathcal{E}(x)\rangle_{\Sigma_0} = [\mathfrak{d}\mathcal{E}(0)]^2 + \int_\Xi [(\mathfrak{d}\mathcal{E})'(x)]^2 dx. \tag{20}$$

Using the reproducing property of $\Pi_x^{\{2\}}(\jmath)$, one can obtain

$$\mathcal{E}(x) = \langle \mathcal{E}(\jmath), \Pi_x^{\{2\}}(\jmath)\rangle_{\Sigma_2}, \quad (\mathfrak{d}\mathcal{E})^{(\sigma)}(x) = \langle \mathcal{E}(\jmath), (\mathfrak{d}\Pi_x^{\{2\}})^{(\sigma)}(\jmath)\rangle_{\Sigma_2}, \ \sigma = 0, 1. \tag{21}$$

With the use of the Schwarz inequality, one can obtain

$$\begin{aligned} |(\mathfrak{d}\mathcal{E})^{(\sigma)}(x)| &= \left|\langle \mathcal{E}(x), (\mathfrak{d}\Pi_x^{\{2\}})^{(\sigma)}(x)\rangle_{\Sigma_2}\right| \\ &\le \left\|(\mathfrak{d}\Pi_x^{\{2\}})^{(\sigma)}(x)\right\|_{\Sigma_0}\|\mathcal{E}\|_{\Sigma_2} \\ &\le \mathcal{C}_{\{\sigma\}}\|\mathcal{E}\|_{\Sigma_2}, \ \sigma = 0, 1. \end{aligned} \tag{22}$$

So $\|\mathfrak{d}\mathcal{E}\|_{\Sigma_0}^2 \le (\mathcal{C}_{\{0\}}^2 + \int_\Xi \mathcal{C}_{\{1\}}^2 dx)\|\mathcal{E}\|_{\Sigma_2}^2$ or $\|\mathfrak{d}\mathcal{E}\|_{\Sigma_0} \le \sqrt{\mathcal{C}_{\{0\}}^2 + \mathcal{C}_{\{1\}}^2}\|\mathcal{E}\|_{\Sigma_2}$. By picking out a countable dense subset $\{x_\sigma\}_{\sigma=1}^\infty$ in Ξ, defining $\omega_\sigma(x) = \Pi_{x_\sigma}^{\{1\}}(x)$, and setting $\Theta_\sigma(x) = \mathfrak{d}^*\omega_\sigma(x)$, one can fit the orthogonal function system of $\Sigma_2(\Xi)$. Furthermore, by the Gram–Schmidt process, one can fit the orthonormal function systems $\{\bar{\Theta}_\sigma(x)\}_{\sigma=1}^\infty$ on $\Sigma_2(\Xi)$ as

$$\bar{\Theta}_\sigma(x) = \sum_{\hbar=1}^{\sigma} \mathcal{A}_{\sigma\hbar}\Theta_\hbar(x). \tag{23}$$

Theorem 4. $\{\Theta_\sigma(x)\}_{\sigma=1}^\infty$ is the complete function system of $\Sigma_2(\Xi)$ with

$$\Theta_\sigma(x) = \mathfrak{d}_\jmath \Pi_x^{\{2\}}(\jmath)\big|_{\jmath=x_\sigma}. \tag{24}$$

Proof: First, $\mathfrak{d}_s$ indicates that $\mathfrak{d}$ applies to a function of $\jmath$. Certainly,

$$\begin{aligned} \Theta_\sigma(x) &= \mathfrak{d}^*\omega_\sigma(x) \\ &= \langle \mathfrak{d}^*\omega_\sigma(\jmath), \Pi_x^{\{2\}}(\jmath)\rangle_{\Sigma_2} \\ &= \langle \omega_\sigma(\jmath), \mathfrak{d}_s\Pi_x^{\{2\}}(\jmath)\rangle_{\Sigma_0} \\ &= \mathfrak{d}_\jmath \Pi_x^{\{2\}}(\jmath)\big|_{\jmath=x_\sigma}. \end{aligned} \tag{25}$$

So $\Theta_o(x)$ can be written as $\mathfrak{d}_\jmath \Pi_x^{\{2\}}(\jmath)|_{\jmath=x_o}$ in $\Sigma_2(\Xi)$.

To illustrate more effective properties in $\Sigma_2(\Xi)$, the set $\left\{\Pi_{x_o}^{\{2\}}(x)\right\}_{o=1}^{\infty}$ is linearly independent as $\{c_o\}_{o=1}^{\eta}$ agrees well with $\sum_{o=1}^{\eta} c_o \Pi_{x_o}^{\{2\}}(x) = 0$, and for $l = 1, 2, \cdots, \eta$, taking $\mathcal{E}_k(x)$ in $\Sigma_2(\Xi)$ as $\mathcal{E}_k(x_l) = \delta_{l,k}$, then

$$\begin{aligned} 0 &= \langle \mathcal{E}_k(x), \sum_{o=1}^{\eta} c_o \Pi_{x_o}^{\{2\}}(x)\rangle_{\Sigma_2} \\ &= \sum_{o=1}^{\eta} \mathscr{b}_o \langle \mathcal{E}_k(x), \Pi_{x_o}^{\{2\}}(x)\rangle_{\Sigma_2} \\ &= \sum_{o=1}^{\eta} c_o \mathcal{E}_k(x_o) \\ &= c_o, k = 1, 2, \cdots, \eta. \end{aligned} \tag{26}$$

So $\left\{\Pi_{x_o}^{\{2\}}(x)\right\}_{o=1}^{\eta}$ is linearly independent for each $\eta \geq 1$.

4 Reproducing kernel: Solutions and convergence

This section aims to construct exact and RKHA numeric solutions of Eq. 19, together with some convergence theories, to ensure this analysis is more efficient. Here, $\mathfrak{C}(\Xi, \mathbb{R})$ and $\mathfrak{C}(\Xi \times \mathbb{R}, \mathbb{R})$ indicate a set of continuous maps on the group inside parentheses.

If $\mathcal{E} \in \mathfrak{C}(\Xi, \mathbb{R})$ and $\{\bar{\Theta}_o(x)\}_{o=1}^{\infty}$ are orthonormal, then $\langle \mathcal{E}(x), \bar{\Theta}_o(x)\rangle_{\Sigma_2}$, $o = 1, 2, \cdots$ are the Fourier maps of $\mathcal{E}$ for $\{\bar{\Theta}_o(x)\}_{o=1}^{\infty}$ and its Fourier expansion $\mathcal{E}(x) = \sum_{o=1}^{\infty} \langle \mathcal{E}(x), \bar{\Theta}_o(x)\rangle_{\Sigma_2} \bar{\Theta}_o(x)$, wherein $\{x_o\}_{o=1}^{\infty}$ is dense throughout Ξ.

Theorem 5. Suppose that $\{a_{ok}\}_{(o,k)=(1,1)}^{(\infty,o)}$ are orthogonalization coefficients of $\{\bar{\Theta}_o(x)\}_{o=1}^{\infty}$ and a unique solution of Eq. 19 exists, then the posteriors are accomplished:

1) As $\varkappa \to \infty$, the exact solution, $\mathcal{E}(x)$, of Eqs 1, 2 is as follows:

$$\mathcal{E}(x) = \sum_{o=1}^{\infty} \sum_{k=1}^{o} a_{ok} \bar{\mathfrak{H}}(x_k, \mathcal{E}(x_k)) \bar{\Theta}_o(x). \tag{27}$$

2) The RKHA numeric solution, $\mathcal{E}_\varkappa(x)$, of Eqs 1, 2 is as follows:

$$\mathcal{E}_\varkappa(x) = \sum_{o=1}^{\varkappa} \sum_{k=1}^{o} a_{ok} \bar{\mathfrak{H}}(x_k, \mathcal{E}(x_k)) \bar{\Theta}_o(x). \tag{28}$$

Proof: For the first side: Through Theorem 4, $\{\bar{\Theta}_o(x)\}_{o=1}^{\infty}$ is an orthonormal basis in $\Sigma_2(\Xi)$, which is complete. Using $\sum_{o=1}^{\infty} \langle \mathcal{E}(x), \bar{\Theta}_o(x)\rangle_{\Sigma_2} \bar{\Theta}_o(x)$ as the Fourier expansion concerning $\{\bar{\Theta}_o(x)\}_{o=1}^{\infty}$, one can obtain $\sum_{o=1}^{\infty} \langle \mathcal{E}(x), \bar{\Theta}_o(x)\rangle_{\Sigma_2} \bar{\Theta}_o(x) < \infty$ in $\|\cdot\|_{\Sigma_2}$. So

$$\begin{aligned} \mathcal{E}(x) &= \sum_{o=1}^{\infty} \langle \mathcal{E}(x), \bar{\Theta}_o(x)\rangle_{\Sigma_2} \bar{\Theta}_o(x) \\ &= \sum_{o=1}^{\infty} \langle \mathcal{E}(x), \sum_{k=1}^{o} a_{ok} \Theta_k(x)\rangle_{\Sigma_2} \bar{\Theta}_o(x) \\ &= \sum_{o=1}^{\infty} \sum_{k=1}^{o} a_{ok} \langle \mathcal{E}(x), \mathfrak{d}^*[\mathcal{E}_k](x)\rangle_{\Sigma_2} \bar{\Theta}_o(x) \\ &= \sum_{o=1}^{\infty} \sum_{k=1}^{o} a_{ok} \langle \mathfrak{d}[\mathcal{E}](x), \omega_j(x)\rangle_{\Sigma_0} \bar{\Theta}_o(x) \\ &= \sum_{o=1}^{\infty} \sum_{k=1}^{o} a_{ok} \langle \bar{\mathfrak{H}}(x, \mathcal{E}(x)), \omega_j(x)\rangle_{\Sigma_0} \bar{\Theta}_o(x) \\ &= \sum_{o=1}^{\infty} \sum_{k=1}^{o} a_{ok} \bar{\mathfrak{H}}(x_k, \mathcal{E}(x_k)) \bar{\Theta}_o(x). \end{aligned} \tag{29}$$

For the second side: Because $\sum_{o=1}^{\infty} \langle \mathcal{E}(x), \bar{\Theta}_o(x)\rangle_{\Sigma_2} \bar{\Theta}_o(x) < \infty$ and $\Sigma_2(\Xi)$ are the Hilbert space, one can truncate Eq. 27 using the $\varkappa$-idiom RKHA numeric solution of $\mathcal{E}(x)$ to generate Eq. 28.

Remark 3. Assume that $\|\mathcal{E}_{\varkappa-1}\|_{\Sigma_2} < \infty$ and $\{x_o\}_{o=1}^{\infty}$ are dense throughout Ξ. Then, according to Eqs 27–28, the portrayal effect can be determined as follows:

$$\begin{cases} \mathcal{E}(x) = \sum_{o=1}^{\infty} \mathcal{V}_o \bar{\Theta}_o(x), \\ \mathcal{V}_o = \sum_{k=1}^{o} a_{ok} \bar{\mathfrak{H}}(x_k, \mathcal{E}(x_k)). \end{cases} \tag{30}$$

$$\begin{cases} \mathcal{E}_\varkappa(x) = \sum_{o=1}^{\varkappa} \mathcal{V}_o \bar{\Theta}_o(x), \\ \mathcal{V}_o = \sum_{k=1}^{o} a_{ok} \bar{\mathfrak{H}}(x_k, \mathcal{E}_{k-1}(x_k)). \end{cases} \tag{31}$$

Theorem 6. Assume that $\|\mathcal{E}_{\varkappa-1} - \mathcal{E}\|_{\Sigma_2} \to 0$, $x_\varkappa \to \jmath$ as $\varkappa \to \infty$, $\|\mathcal{E}_{\varkappa-1}\|_{\Sigma_2} < \infty$, and $\bar{\mathfrak{H}}(x, \mathcal{E}(x)) \in \mathfrak{C}(\Xi \times \mathbb{R}, \mathbb{R})$. Then, $\bar{\mathfrak{H}}(x_\varkappa, \mathcal{E}_{\varkappa-1}(x_\varkappa)) \to \bar{\mathfrak{H}}(\jmath, \mathcal{E}(\jmath))$ as $\varkappa \to \infty$.

Proof: It all started where $\mathcal{E}_{\varkappa-1}(x_\varkappa) \to \mathcal{E}(\jmath)$ as $\varkappa \to \infty$. Evidently, one can obtain

$$\begin{aligned} |\mathcal{E}_{\varkappa-1}(x_\varkappa) - \mathcal{E}(\jmath)| &= |\mathcal{E}_{\varkappa-1}(x_\varkappa) - \mathcal{E}_{\varkappa-1}(\jmath) + \mathcal{E}_{\varkappa-1}(\jmath) - \mathcal{E}(\jmath)| \\ &\leq |\mathcal{E}_{\varkappa-1}(x_\varkappa) - \mathcal{E}_{\varkappa-1}(\jmath)| + |\mathcal{E}_{\varkappa-1}(\jmath) - \mathcal{E}(\jmath)| \\ &\leq |(\mathcal{E}_{\varkappa-1})'(\sigma)||x_\varkappa - \jmath| + |\mathcal{E}_{\varkappa-1}(\jmath) - \mathcal{E}(\jmath)|, \end{aligned} \tag{32}$$

with σ in between $x_\varkappa$ and $\jmath$. Applying Theorem 2, one can obtain $|\mathcal{E}_{\varkappa-1}(\jmath) - \mathcal{E}(\jmath)| \leq 3.5\|\mathcal{E}_{\varkappa-1} - \mathcal{E}\|_{\Sigma_2}$ or equivalently $|\mathcal{E}_{\varkappa-1}(\jmath) - y(\jmath)| \to 0$ as $\varkappa \to \infty$ and $|(\mathcal{E}_{\varkappa-1})'(\sigma)| \leq 3\|\mathcal{E}_{\varkappa-1}\|_{\Sigma_2}$. Using $\|\mathcal{E}_{\varkappa-1}\|_{\Sigma_2} < \infty$ and $x_\varkappa \to \jmath$, one can obtain equivalently $|\mathcal{E}_{\varkappa-1}(x_\varkappa) - \mathcal{E}_{\varkappa-1}(\jmath)| \to 0$ as $\varkappa \to \infty$. By $\bar{\mathfrak{H}}(x, \mathcal{E}(x)) \in \mathfrak{C}(\Xi \times \mathbb{R}, \mathbb{R})$, it gives a glimpse that $\bar{\mathfrak{H}}(x_\varkappa, \mathcal{E}_{\varkappa-1}(x_\varkappa)) \to \bar{\mathfrak{H}}(\jmath, u(\jmath))$ as $\varkappa \to \infty$.

Theorem 7. One gains $\mathcal{E}_\varkappa(x) \to \mathcal{E}(x)$ as $\varkappa \to \infty$.

Proof: Because $\mathcal{E}_{\varkappa+1}(x) = \mathcal{E}_\varkappa(x) + \mathcal{V}_{\varkappa+1}\bar{\Theta}_{\varkappa+1}(x)$ and the orthogonality of $\{\bar{\Theta}_\varrho(x)\}_{\varrho=1}^{\infty}$, one can obtain

$$\begin{aligned}\|\mathcal{E}_{\varkappa+1}\|_{\Sigma_2}^2 &= \|\mathcal{E}_\varkappa\|_{\Sigma_2}^2 + \mathcal{V}_{\varkappa+1}^2\\ &= \|\mathcal{E}_{\varkappa-1}\|_{\Sigma_2}^2 + \mathcal{V}_\varkappa^2 + \mathcal{V}_{\varkappa+1}^2\\ &= \vdots\\ &= \|\mathcal{E}_0\|_{\Sigma_2}^2 + \sum_{\varrho=1}^{\varkappa+1}\mathcal{V}_\varrho^2.\end{aligned} \tag{33}$$

So $\|\mathcal{E}_{\varkappa+1}\|_{\Sigma_2} \geq \|\mathcal{E}_\varkappa\|_{\Sigma_2}$ and $\exists \kappa \in \mathbb{R}$ such that $\sum_{\varrho=1}^{\infty}\mathcal{V}_\varrho^2 = \kappa$ or $\{\mathcal{V}_\varrho^2\}_{\varrho=1}^{\infty} \in l^2$. To get

$$\mathcal{E}_\lambda(x) - \mathcal{E}_{\lambda-1}(x) \perp \mathcal{E}_{\lambda-1}(x) - \mathcal{E}_{\lambda-2}(x) \perp \cdots \perp \mathcal{E}_{\varkappa+1}(x) - \mathcal{E}_\varkappa(x), \tag{34}$$

it is adequate to have for $\lambda > \varkappa$ that

$$\begin{aligned}\|\mathcal{E}_\lambda - \mathcal{E}_\varkappa\|_{\Sigma_2}^2 &= \|\mathcal{E}_\lambda - \mathcal{E}_{\lambda-1} + \mathcal{E}_{\lambda-1} - \cdots + \mathcal{E}_{\varkappa+1} - \mathcal{E}_\varkappa\|_{\Sigma_2}^2\\ &= \|\mathcal{E}_\lambda - \mathcal{E}_{\lambda-1}\|_{\Sigma_2}^2 + \|\mathcal{E}_{\lambda-1} - \mathcal{E}_{\lambda-2}\|_{\Sigma_2}^2 + \cdots + \|\mathcal{E}_{\varkappa+1} - \mathcal{E}_\varkappa\|_{\Sigma_2}^2,\end{aligned} \tag{35}$$

with $\|\mathcal{E}_\lambda - \mathcal{E}_{\lambda-1}\|_{\Sigma_2}^2 = \mathcal{V}_\lambda^2$. However, on the other line, $\|\mathcal{E}_\lambda - \mathcal{E}_\varkappa\|_{\Sigma_2}^2 = \sum_{l=\varkappa+1}^{\lambda}\mathcal{V}_\varrho^2 \to 0$ as $\varkappa, \lambda \to \infty$. Using completeness, $\exists \mathcal{E}_\varkappa(x) \in \Sigma_2(\Xi)$ such that $\mathcal{E}_\varkappa(x) \to \mathcal{E}(x)$ as $\varkappa \to \infty$.

Theorem 8. Assume that $\|\mathcal{E}_{\varkappa-1}\|_{\Sigma_2} < \infty$ and $\{x_\varrho\}_{\varrho=1}^{\infty}$ are dense throughout Ξ. Then, $\mathcal{E}(x) = \sum_{\varrho=1}^{\infty}\mathcal{V}_\varrho\bar{\Theta}_\varrho(x)$ as $\varkappa \to \infty$.

Proof: Applying $\lim_{\varkappa \longrightarrow \infty}$ on Eq. 31, one gets $\mathcal{E}(x) = \sum_{\varrho=1}^{\infty}\mathcal{V}_\varrho\bar{\Theta}_\varrho(x)$. So

$$\begin{aligned}\mathfrak{A}[\mathcal{E}](x_\hbar) &= \sum_{\varrho=1}^{\infty}\mathcal{V}_\varrho\langle\mathfrak{A}[\bar{\Theta}_\varrho](x), \omega_\hbar(x)\rangle_{\Sigma_0}\\ &= \sum_{\varrho=1}^{\infty}\mathcal{V}_\varrho\langle\bar{\Theta}_\varrho(x), \mathfrak{A}^*[\mathfrak{S}_\hbar](x)\rangle_{\Sigma_2},\\ &= \sum_{\varrho=1}^{\infty}\mathcal{V}_\varrho\langle\bar{\Theta}_\varrho(x), \Theta_\hbar(x)\rangle_{\Sigma_2}.\end{aligned} \tag{36}$$

$$\begin{aligned}\sum_{\hbar=1}^{l}\mathfrak{a}_{l\hbar}\mathfrak{A}[\Theta](x_\hbar) &= \sum_{\varrho=1}^{\infty}\mathcal{V}_\varrho\langle\bar{\Theta}_\varrho(x), \sum_{\hbar=1}^{l}\mathfrak{a}_{l\hbar}\Theta_\hbar(x)\rangle_{\Sigma_2}\\ &= \sum_{\varrho=1}^{\infty}\mathcal{V}_\varrho\langle\bar{\Theta}_\varrho(x), \bar{\Theta}_l(x)\rangle_{\Sigma_2}\\ &= \mathcal{V}_l.\end{aligned} \tag{37}$$

Sequentially, if $l = 1$, then $\mathfrak{A}[\mathcal{E}](x_1) = \bar{\mathfrak{H}}(x_1, \mathcal{E}_0(x_1))$, and if $l = 2$, then $\mathfrak{A}[\mathcal{E}](x_2) = \bar{\mathfrak{H}}(x_2, \mathcal{E}_1(x_2))$. As a rule, one can obtain $\mathfrak{A}[\mathcal{E}](x_\varkappa) = \bar{\mathfrak{H}}(x_\varkappa, \mathcal{E}_{\varkappa-1}(x_\varkappa))$. By the condition of density, $\forall x \in \Xi$; $\exists\{x_{\varkappa_q}\}_{q=1}^{\infty}$ such that $x_{\varkappa_q} \to x$ as $q \to \infty$ or equivalently $\mathfrak{A}[\mathcal{E}](x_{\varkappa_q}) = \bar{\mathfrak{H}}(x_{\varkappa_q}, \mathcal{E}_{\varkappa_q-1}(x_{\varkappa_q}))$. Letting $q \to \infty$, one gets $\mathfrak{A}[\mathcal{E}](x) = \bar{\mathfrak{H}}(\mathcal{E}, \mathcal{E}(x))$. Because $\bar{\Theta}_\varrho(x) \in \Sigma_2(\Xi)$, $\mathcal{E}(x)$ fulfills (Eq. 19).

5 Error: Estimation and bound

As a matter of fact, the exact solution of FDMs (Eqs 1, 2) restricted with the CFD depends on α and β. In most cases, this real problem is complicated to be solved traditionally because it lacks an exact solution. This induces us to develop numerical schemes like RKHA that generate approximated realizations of the exact solution depending on the values of α and β.

Here, we will fix $\mathcal{T} = \{x_\varrho\}_{\varrho=1}^{\varkappa} \subset \Xi - \{0, 1\}$ with $x_1 \leq x_2 \leq \cdots \leq x_\varkappa \subseteq \Xi$, $\hbar = \max_{0\leq\varrho\leq\varkappa}|x_{\varrho+1} - x_\varrho|$, $\|\wp\|_\infty = \max_{x\in[x_\varrho, x_{\varrho+1}]}|\wp(x)|$, and $\|\mathfrak{A}^{-1}\| = \sup_{0\neq\mathcal{E}\in\Sigma_2}\|\mathcal{E}\|_{\Sigma_0}^{-1}\|\mathfrak{A}^{-1}\|_{\Sigma_2}$. Furthermore, we will fix $RE_\varkappa(x) = \mathfrak{A}[\mathcal{E}_\varkappa](x) - \bar{\mathfrak{H}}(x, \mathcal{E}(x))$ to the residual truncated error at $x \in \Xi$.

Lemma 1. One gains $\mathfrak{A}[\mathcal{E}_\varkappa](x_j) = \mathfrak{A}\mathcal{E}(x_j)$, $x_j \in \mathcal{T}$.

Proof: Set $\Pi_\varkappa$: $\Sigma_2(\Xi) \to \left\{\sum_{j=1}^{\varkappa}\mathscr{b}_j\mathcal{E}_j(x), \mathscr{b}_j \in \mathbb{R}\right\}$. So

$$\begin{aligned}\mathfrak{A}[\mathcal{E}_\varkappa]\left(x_j\right) &= \langle\mathcal{E}_\varkappa(x), \mathfrak{a}_{x_\hbar}\Pi_{x_\hbar}^{\{2\}}(x)\rangle_{\Sigma_2}\\ &= \langle\mathcal{E}_\varkappa(x), \mathcal{E}_\hbar(x)\rangle_{\Sigma_2}\\ &= \langle\Pi_\varkappa\mathcal{E}(x), \mathcal{E}_j(x)\rangle_{\Sigma_2}\\ &= \langle\mathcal{E}(x), \Pi_\varkappa\mathcal{E}_j(x)\rangle_{\Sigma_2}\\ &= \langle\mathcal{E}(x), \mathcal{E}_j(x)\rangle_{\Sigma_2}\\ &= \langle\mathcal{E}(x), \mathfrak{a}_{x_j}\Pi_{x_j}^{\{2\}}(x)\rangle_{\Sigma_2}\\ &= \mathfrak{a}_{x_j}\langle\mathcal{E}(x), \Pi_{x_j}^{\{2\}}(x)\rangle_{\Sigma_2}\\ &= \mathfrak{a}_{x_j}\mathcal{E}\left(x_j\right)\\ &= \mathfrak{A}\mathcal{E}\left(x_j\right).\end{aligned} \tag{38}$$

In other words, $\mathfrak{A}[\mathcal{E}_\varkappa](x_j) = \mathfrak{A}\mathcal{E}(x_j)$.

Lemma 2. Assume that $\wp \in \mathfrak{C}^\lambda(\Xi, \mathbb{R})$, $\wp^{(\lambda+1)} \in L^2(\Xi)$ for a fixed $\lambda \geq 1$, and $\wp \to 0$ at $\mathcal{T}$ with $\varkappa \geq \lambda + 1$. So $\wp \in \Sigma_0(\Xi)$ and a parameter $\mathcal{A}$ exist with

$$\|\wp\|_{\Sigma_0} \leq \mathcal{A}\hbar^\lambda\max_{x\in\Xi}|\wp^{(\lambda+1)}(x)|. \tag{39}$$

Proof: Clearly, $\wp \in \Sigma_0(\Xi)$ and $\forall x \in [x_\varrho, x_{\varrho+1}]$, $\varrho = 1, 2, \cdots\varkappa$, one can obtain

$$\begin{aligned}|\wp(x)| &= |\wp(x) - \wp(\tau_\varrho)|\\ &= \left|\int_{\tau_\varrho}^{x}\wp'(\tau)d\tau\right|\\ &\leq |x - \tau_\varrho|\max_{x\in[x_\varrho, x_{\varrho+1}]}|\wp'(x)|,\\ &\leq \hbar\|\wp'\|_\infty.\end{aligned} \tag{40}$$

On $[x_\varrho, x_{\varrho+1}]$, applying Roll's theorem on $\wp$ yields $\wp'(\tau_\varrho) = 0$ with $\tau_\varrho \in (x_\varrho, x_{\varrho+1})$, $\varrho = 1, 2, \cdots, \varkappa - 1$. So for fixed x, $\exists\tau_\varrho$ such that $|x - \tau_\varrho| < 2\hbar$. Similarly, one can write

$$\begin{aligned}|\wp'(x)| &= |\wp'(x) - \wp'(\tau_\varrho)|\\ &= \left|\int_{\tau_\varrho}^{x}\wp''(\tau)d\tau\right|\\ &\leq |x - \tau_\varrho|\max_{x\in[x_\varrho, x_{\varrho+1}]}|\wp''(x)|,\\ &\leq 2\hbar\|\wp''\|_\infty.\end{aligned} \tag{41}$$

So $|\wp(x)| \leq 2\hbar^2\|\wp''\|_\infty$. Sequentially, a parameter C_1 exists with $|\wp(x)| \leq C_1\hbar^{\lambda+1}\|\wp^{(\lambda+1)}\|_\infty$ and $|\wp'(x)| \leq C_1\hbar^\lambda\|\wp^{(\lambda+1)}\|_\infty$. By compiling the previous results, one can obtain

$$\begin{aligned}\|\wp\|_{\Sigma_0} &= \left((\wp(0))^2 + \int_\Xi(\wp'(\tau))^2d\tau\right)^{\frac{1}{2}}\\ &\leq \mathcal{A}\hbar^\lambda\max_{x\in\Xi}|\wp^{(\lambda+1)}(x)|,\end{aligned} \tag{42}$$

with $\mathcal{A} = C_1\sqrt{\hbar+1}$.

Theorem 9. A parameter $\mathcal{B}$ exists with

$$\left\|\mathcal{E}^{(\sigma)} - \mathcal{E}_{\varkappa}^{(\sigma)}\right\|_{\infty} \le \mathcal{B}\hbar^{\lambda}\max_{x\in\Xi}\left|RE_{\varkappa}^{(\lambda+1)}(x)\right|, \sigma = 0,1,2. \tag{43}$$

Proof: Utilizing Lemma 3, one can obtain

$$\|RE_{\varkappa}\|_{W_2^1} \le \mathcal{A}\hbar^{\lambda}\max_{x\in\Xi}\left|RE_{\varkappa}^{(\lambda+1)}(x)\right|. \tag{44}$$

However, since $RE_{\varkappa}(x) = \mathfrak{d}\mathcal{E}_{\varkappa}(x) - \bar{\mathfrak{H}}(\mathcal{E},\mathcal{E}(x)) = \mathfrak{d}(\mathcal{E}_{\varkappa}(x) - \mathcal{E}(x))$, then $\mathcal{E} - \mathcal{E}_{\varkappa} = \mathfrak{d}^{-1}RE_{\varkappa}$ and a parameter C_2 exists with

$$\begin{aligned}\|\mathcal{E} - \mathcal{E}_{\varkappa}\|_{\Sigma_2} &= \left\|\mathfrak{d}^{-1}RE_{\varkappa}\right\|_{\Sigma_2}\\ &\le \left\|\mathfrak{d}^{-1}\right\|\|RE_{\varkappa}\|_{\Sigma_0}\\ &\le \mathcal{A}C_2\hbar^{\lambda}\max_{x\in\Xi}\left|RE_{\varkappa}^{(\lambda+1)}(x)\right|.\end{aligned} \tag{45}$$

Applying Theorem 2, one can obtain

$$\begin{aligned}\left|\mathcal{E}^{(\sigma)} - \mathcal{E}_{\varkappa}^{(\sigma)}\right| &\le C_3\|\mathcal{E} - \mathcal{E}_{\varkappa}\|_{\Sigma_2}\\ &\le \mathcal{A}C_2C_3\hbar^{\lambda}\max_{x\in\Xi}\left|RE_{\varkappa}^{(\lambda+1)}(x)\right|, \sigma = 0,1,2.\end{aligned} \tag{46}$$

In another mode, one can obtain $\|\mathcal{E}^{(\sigma)} - \mathcal{E}_{\varkappa}^{(\sigma)}\|_{\infty} \le \mathcal{B}\hbar^{\lambda}\max_{x\in\Xi}|RE_{\varkappa}^{(\lambda+1)}(x)|$, $\sigma = 0,1,2$, where $\mathcal{B} = \mathcal{A}C_2C_3$.

Ultimately, one can see that $\|\mathcal{E} - \mathcal{E}^{\varkappa}\|_{\Sigma_2}^2$ is decreasing for a large $\varkappa$ as

$$\begin{aligned}\|\mathcal{E} - \mathcal{E}^{\varkappa}\|_{\Sigma_2}^2 - \left\|\mathcal{E} - \mathcal{E}^{\varkappa-1}\right\|_{\Sigma_2}^2 &= \left\|\sum_{\sigma=\varkappa+1}^{\infty}\langle\mathcal{E}(x),\bar{\Theta}_{\sigma}(x)\rangle_{\mathcal{A}}\bar{\Theta}_{\sigma}(x)\right\|_{\Sigma_2}^2\\ &\quad - \left\|\sum_{\sigma=\varkappa}^{\infty}\langle\mathcal{E}(x),\bar{\Theta}_{\sigma}(x)\rangle_{\Sigma_2}\bar{\Theta}_{\sigma}(x)\right\|_{\Sigma_2}^2\\ &= \sum_{\sigma=\varkappa+1}^{\infty}\langle\mathcal{E}(x),\bar{\Lambda}_{\sigma}(l)\rangle_{\Sigma_2}^2\\ &\quad - \sum_{\sigma=\varkappa}^{\infty}\langle\mathcal{E}(x),\bar{\Theta}_{\sigma}(x)\rangle_{\Sigma_2}^2 < 0.\end{aligned} \tag{47}$$

However, as $\sum_{\sigma=1}^{\infty}\langle\mathcal{E}(x),\bar{\Theta}_{\sigma}(x)\rangle_{\Sigma_2}\bar{\Theta}_{\sigma}(x) < \infty$, one can obtain $\|\mathcal{E} - \mathcal{E}^{\varkappa}\|_{\Sigma_2}^2 \to 0$ as $\varkappa \to \infty$.

6 Justifications: Algorithms, applications, and analyses

To clarify the portability and effectiveness of the presented numeric approach, we need some of the steps, the first of which is to provide sufficient algorithms to demonstrate the mechanism of the solution, the second of which is to present several tangible applications, and then finally to provide several tables, figures, and numeric explanations of the solution procedures. However, all of this is the content of the following sections.

6.1 Algorithms

Next, three used algorithms in our RKHA implementation are given. These algorithms are problem initialization, the Gram–Schmidt process, and RKHA solution steps, simultaneously. However, an expert in the Mathematica platform can interpret these steps in the form of programs.

Stride 1: Set the assumptions.

$$\mathcal{E}(x): \to \mathcal{E}(x) - \left(\frac{1}{2}\Gamma(3-\alpha)\mathcal{E}_1^{\alpha}x^2 + \mathcal{E}_0\right), \tag{48}$$

$$\begin{aligned}\bar{\mathfrak{H}}(x,\mathcal{E}(x)) \coloneqq &\left(\frac{\Gamma(3-\alpha)}{\Gamma(3-\alpha-\beta)} + \mu\frac{\Gamma(3-\alpha)}{\Gamma(3-\beta)}x^{\alpha}\right)\mathcal{E}_1^{\alpha}x^{2-\alpha-\beta}\\ &+ \mathfrak{H}(x,\mathcal{E}(x) - 0.5\Gamma(3-\alpha)\mathcal{E}_1^{\alpha}x^2 - \mathcal{E}_0).\end{aligned} \tag{49}$$

Output: Homogenous FLM.

$$\frac{\partial^{\beta}}{\partial x}\left(\frac{\partial^{\alpha}}{\partial x} + \mu\right)\mathcal{E}(x) = \bar{\mathfrak{H}}(x,\mathcal{E}(x)), \tag{50}$$

$$\begin{cases}\mathcal{E}(0) = 0,\\ \dfrac{\partial^{\alpha}}{\partial x}\mathcal{E}(1) = 0.\end{cases} \tag{51}$$

Stride 2: Define a suitable operator.

$$\mathfrak{d}\colon \Sigma_2(\Xi) \to \Sigma_0(\Xi), \tag{52}$$

$$\mathfrak{d}[\mathcal{E}](x) \coloneqq \frac{\partial^{\beta}}{\partial x}\left(\frac{\partial^{\alpha}}{\partial x} + \mu\right)\mathcal{E}(x). \tag{53}$$

Output: Homogenous FLM in the functional form.

$$\begin{cases}\mathfrak{d}[\mathcal{E}](x) \coloneqq \bar{\mathfrak{H}}(x,\mathcal{E}(x)),\\ \mathcal{E}(0) = 0,\\ \dfrac{\partial^{\alpha}}{\partial x}\mathcal{E}(1) = 0.\end{cases} \tag{54}$$

Algorithm 1. Problem initialization.

Stride 1: At $\sigma \ge 2$ and $\hbar = 1,2,\ldots,\sigma-1$, evaluate

$$\begin{aligned}a_{11} &= \frac{1}{\|\Theta_1\|_{\Sigma_2}},\\ a_{\sigma\sigma} &= \frac{1}{\sqrt{\|\Theta_{\sigma}\|_{\Sigma_2}^2 - \sum_{p=1}^{\sigma-1}\langle\Theta_{\sigma}(x),\bar{\Theta}_p(x)\rangle_{\Sigma_2}^2}}, \sigma \ne 1\\ a_{\sigma\hbar} &= -\frac{1}{\sqrt{\|\Theta_{\sigma}\|_{\Sigma_2}^2 - \sum_{p=1}^{\sigma-1}\langle\Theta_{\sigma}(x),\bar{\Theta}_p(x)\rangle_{\Sigma_2}^2}}\sum_{p=\hbar}^{\sigma-1}\langle\Theta_{\sigma}(x),\\ &\quad \bar{\Theta}_p(x)\rangle_{\Sigma_2}\varepsilon_{pj}, \sigma > \hbar\end{aligned} \tag{55}$$

Output: $a_{\sigma\hbar}$ parameters.

Stride 2: At $\mathscr{o} = 1, 2, 3, \ldots$, evaluate

$$\bar{\Theta}_{\mathscr{o}}(x) = \sum_{j=1}^{\mathscr{o}} \mathscr{a}_{\mathscr{o}\mathscr{k}} \Theta_{\mathscr{o}}(x). \tag{56}$$

Output: $\{\bar{\Theta}_{\mathscr{o}}(x)\}_{\mathscr{o}=1}^{\infty}$ system.

Algorithm 2. Gram–Schmidt process.

Stride I: At fix $l, \mathscr{k}$ on Ξ evaluating $x_{\mathscr{o}} = 1/x\mathscr{o}$ and $\Theta_{\mathscr{o}}(x) = \mathfrak{A}^{*}[\omega_{\mathscr{o}}](x)$ in $\mathscr{o} = 1, 2, \cdots, \varkappa$.

Output: $\Theta_{\mathscr{o}}(x)$ system.

Stride II: Wherein $\mathscr{o} \geq 1$ and $j = 1, 2, \cdots, \mathscr{o} - 1$, evaluate Gram–Schmidt.

Output: $\mathscr{a}_{\mathscr{o}\mathscr{k}}$ parameters.

Stride III: Set $\bar{\Theta}_{\mathscr{o}}(x) = \sum_{j=1}^{\mathscr{o}} \mathscr{a}_{\mathscr{o}\mathscr{k}} \Theta_{\mathscr{o}}(x)$ in $\mathscr{o} = 1, 2, \cdots, \varkappa$.

Output: $\bar{\Theta}_{\mathscr{o}}(x)$ system.

Stride IV: Set $\mathcal{E}_0(x_0) = 0$ in $\mathscr{o} = 1, 2, \cdots, \varkappa$ and evaluate

$$\begin{aligned} \mathcal{E}_{\mathscr{o}}(x_{\mathscr{o}}) &= \mathcal{E}_{\mathscr{o}-1}(x_{\mathscr{o}}), \\ \mathcal{V}_{\mathscr{o}} &= \sum_{\mathscr{k}=1}^{\mathscr{o}} \mathscr{a}_{\mathscr{o}\mathscr{k}} \bar{\mathfrak{H}}(x_{\mathscr{k}}, \mathcal{E}(x_{\mathscr{k}})), \\ \mathcal{E}_{\varkappa}(x_{\mathscr{o}}) &= \sum_{\mathscr{k}=1}^{\mathscr{o}} \mathcal{V}_{\mathscr{o}} \bar{\Theta}_{\mathscr{k}}(x). \end{aligned} \tag{57}$$

Output: $\varkappa$-term numeric approximation $\mathcal{E}_{\varkappa}(x_{\mathscr{o}})$ of $\mathcal{E}(x_{\mathscr{o}})$.

Algorithm 3. Process of RKHA solutions.

6.2 Applications

Next, three test applications that coincide with the FLM platform are utilized on the basis of the CFD: the first is $(\alpha, \beta) = (1/2, 4/5)$, the second is $(\alpha, \beta) = (1/3, 3/4)$, and the third is $(\alpha, \beta) = (1/4, 4/5)$. Actually, these applications are solved and analyzed using the presented RKHA as utilized in Algorithm 1, Algorithm 2, Algorithm 3.

Application 1: Theorize the posterior and evaluate $\mathcal{E}_{\varkappa}(x_{\mathscr{o}})$:

$$\frac{\partial^{\frac{4}{5}}}{\partial x}\left(\frac{\partial^{\frac{1}{2}}}{\partial x} + 1\right)\mathcal{E}(x) = \frac{25}{3\Gamma\left(\frac{1}{5}\right)} x^{\frac{6}{5}} + \frac{2}{\Gamma\left(\frac{17}{10}\right)} x^{\frac{7}{10}}, \tag{58}$$

equipped with the posterior boundary condition:

$$\begin{cases} \mathcal{E}(0) = 0, \\ \dfrac{\partial^{\frac{1}{2}}}{\partial x}\mathcal{E}(1) - \dfrac{8}{3\sqrt{\pi}} = 0. \end{cases} \tag{59}$$

Here, $\mathcal{E}(x) = x^2$ is the exact smooth solution of Eqs 58, 59 on Ξ.

Application 2: Theorize the posterior and evaluate $\mathcal{E}_{\varkappa}(x_{\mathscr{o}})$:

$$\frac{\partial^{\frac{3}{4}}}{\partial x}\left(\frac{\partial^{\frac{1}{3}}}{\partial x} + 1\right)\mathcal{E}(x) + \ln(\mathcal{E}(x)) = 2e^{x} - \frac{\Gamma\left(\frac{1}{4}, x\right)}{\Gamma\left(\frac{1}{4}\right)} e^{x} - \frac{\Gamma\left(\frac{11}{12}, x\right)}{\Gamma\left(\frac{11}{12}\right)} e^{x} + x, \tag{60}$$

equipped with the posterior boundary condition:

$$\begin{cases} \mathcal{E}(0) = 0, \\ \dfrac{\partial^{\frac{1}{3}}}{\partial x}\mathcal{E}(1) - \left(1 - \dfrac{\Gamma\left(\frac{2}{3}, 1\right)}{\Gamma\left(\frac{2}{3}\right)}\right) e = 0. \end{cases} \tag{61}$$

Here, $\mathcal{E}(x) = e^{x}$ is the exact smooth solution of Eqs 60, 61 on Ξ.

Application 3: Theorize the posterior and evaluate $\mathcal{E}_{\varkappa}(x_{\mathscr{o}})$:

$$\frac{\partial^{\frac{4}{5}}}{\partial x}\left(\frac{\partial^{\frac{1}{4}}}{\partial x} + \mu\right)\mathcal{E}(x) + \sqrt[3]{\mathcal{E}(x)} = \frac{25}{3\Gamma\left(\frac{1}{5}\right)} x^{\frac{6}{5}} + \frac{2}{\Gamma\left(\frac{39}{20}\right)} x^{\frac{19}{20}}, \tag{62}$$

equipped with the posterior boundary condition:

$$\begin{cases} \mathcal{E}(0) = 0, \\ \dfrac{\partial^{\frac{1}{4}}}{\partial x}\mathcal{E}(1) - \dfrac{32}{21\Gamma\left(\frac{3}{4}\right)} = 0. \end{cases} \tag{63}$$

Here, $\mathcal{E}(x) = (x^{1/2} + x^{4/3})^3$ is the exact smooth solution of (Eqs 62, 63) on Ξ.

6.3 Analyses

Eventually, to clarify the portability and effectiveness of the presented RKHA, we present and provide several RKHA solution tables, RKHA numeric solution figures, RKHA absolute error figures, and RKHA relative error figures. However, in this section, we used $x_{\mathscr{o}} = \mathscr{o} - 1/\varkappa - 1$ with $\mathscr{o} = 1, 2, \cdots, \varkappa = 101$ in $\mathcal{E}_{\varkappa}(x_{\mathscr{o}})$ on Ξ and then executed Algorithm 3 throughout and its related steps.

The tabulated data presenting

$$\begin{aligned} &(x_{\mathscr{o}}, \mathcal{E}(x_{\mathscr{o}})), \\ &(x_{\mathscr{o}}, \mathcal{E}_{\varkappa}(x_{\mathscr{o}})), \\ &\rho_{\varkappa}(x_{\mathscr{o}}) = |\mathcal{E}(x_{\mathscr{o}}) - \mathcal{E}_{\varkappa}(x_{\mathscr{o}})|, \\ &\sigma_{\varkappa}(x_{\mathscr{o}}) = |\mathcal{E}(x_{\mathscr{o}}) - \mathcal{E}_{\varkappa}(x_{\mathscr{o}})|\mathcal{E}^{-1}(x_{\mathscr{o}}), \end{aligned} \tag{64}$$

concerning the features of the memory inherited, are utilized in detail by the RKHA performance of the applications addressed previously, as shown in the included tables (Tables 1–3).

The 2-D Cartesian plots presenting $(x_{\mathscr{o}}, \mathcal{E}(x_{\mathscr{o}}))$, concerning the features of the memory inherited, are utilized in detail by the RKHA performance of the applications addressed previously, as shown in the included graphs (Figures 1A–C).

The 2-D Cartesian plots presenting $(x_{\mathscr{o}}, \rho_{\varkappa}(x_{\mathscr{o}}))$, concerning the features of the memory inherited, are utilized in detail by the RKHA performance of the applications addressed previously, as shown in the included graphs (Figures 2A–C).

Ultimately, the 2-D Cartesian plots presenting $(x_{\mathscr{o}}, \sigma_{\varkappa}(x_{\mathscr{o}}))$, concerning the features of the memory inherited, are utilized in detail by the RKHA performance of the applications addressed previously, as shown in the included graphs (Figures 3A–C).

7 Outline: Conclusion and outlook

This research embraced the RKHA to handle a type of well-known FDM called FLM on the basis of the CFD by including three test applications. A detailed presentation of the theories related to the establishment of the solution and the formulation of the approximate was interspersed with the construction of the necessary spaces and the associations' form of Green's functions used, with many new results that centered on convergence, error, and independence. Based on the RKHA, $\mathcal{E}(x_o)$, $\mathcal{E}_\varkappa(x_o)$, $\rho_\varkappa(x_o)$, and $\sigma_\varkappa(x_o)$ have been sketched in 2-D and tabulated for various value parameters of (α,β) and x_o. Conclusively, obtaining analytical solutions for many types of FDMs is not a simple procedure, which motivates us to conduct more studies and scientific research to obtain innovative approximations of FDMs subject to influence the CFD. The RKHA has diverse feasible and favorable benefits. First, the RKHA is appropriate and delicate since the approximation is very closest to the required solution. Second, by utilizing small $\varkappa$ terms, we can obtain high accuracy. Third, it is an easy, simple, and soft method to be applied since it does not require sophisticated mathematical tools or an adept professional programmer. Fourth, it is global since it may be utilized to handle different types of fractional complex models. Fifth, the main characteristic of the RKHA is that it may be used with other orthogonal basis sequences. Our outlook study will focus on solving the FLM concerning fuzzy boundaries.

Data availability statement

The original contributions presented in the study are included in the article/Supplementary Material; further inquiries can be directed to the corresponding author.

Author contributions

MA: data curation, investigation, software, methodology, validation, roles/writing—original draft, and writing—review and editing. OA: funding acquisition, investigation, resources, supervision, visualization, and roles/writing—original draft. BM: conceptualization, formal analysis, investigation, project administration, software, and writing—review and editing.

Acknowledgments

The authors are grateful to the Middle East University, Amman, Jordan for the financial support granted to cover the publication fee of this research article.

Conflict of interest

The authors declare that the research was conducted in the absence of any commercial or financial relationships that could be construed as a potential conflict of interest.

Publisher's note

All claims expressed in this article are solely those of the authors and do not necessarily represent those of their affiliated organizations, or those of the publisher, the editors, and the reviewers. Any product that may be evaluated in this article, or claim that may be made by its manufacturer, is not guaranteed or endorsed by the publisher.

References

1. Baghani O. On fractional Langevin equation involving two fractional orders. *Commun Nonlinear Sci Numer Simulation* (2017) 42:675–81. doi:10.1016/j.cnsns.2016.05.023

2. Salem A, Mshary N. On the existence and uniqueness of solution to fractional-order Langevin equation. *Adv Math Phys* (2020) 2020:–11. doi:10.1155/2020/8890575

3. Salem A, Alnegga M. Fractional Langevin equations with multi-point and non-local integral boundary conditions. *Cogent Math Stat* (2020) 7:1758361. doi:10.1080/25742558.2020.1758361

4. Sudsutad W, Ntouyas SK, Tariboon J. Systems of fractional Langevin equations of Riemann-Liouville and Hadamard types. *Adv Differ Equ* (2015) 2015:235. doi:10.1186/s13662-015-0566-8

5. Yadav S, Kumar D, Nisar KS. A reliable numerical method for solving fractional reaction-diffusion equations. *J King Saud Univ – Sci* (2021) 33:101320. doi:10.1016/j.jksus.2020.101320

6. Fang D, Li L. Numerical approximation and fast evaluation of the overdamped generalized Langevin equation with fractional noise. *Math Model Numer Anal* (2020) 54:431–63. doi:10.1051/m2an/2019067

7. Fazli H, Sun HG, Nieto JJ. Fractional Langevin equation involving two fractional orders: Existence and uniqueness revisited. *Mathematics* (2020) 8:743. doi:10.3390/math8050743

8. Guo P, Zeng C, Li C, Chen YQ. Numerics for the fractional Langevin equation driven by the fractional Brownian motion. *Fract Calc Appl Anal* (2013) 16:123–41. doi:10.2478/s13540-013-0009-8

9. Mainardi F. *Fractional calculus and waves in linear viscoelasticity*. UK: Imperial College Press (2010).

10. Zaslavsky GM. *Hamiltonian chaos and fractional dynamics*. UK: Oxford University Press (2005).

11. Podlubny I. *Fractional differential equations*. USA: Academic Press (1999).

12. Samko SG, Kilbas AA, Marichev OI. *Fractional integrals and derivatives theory and applications*. USA: Gordon & Breach (1993).

13. Kilbas A, Srivastava H, Trujillo J. *Theory and applications of fractional differential equations*. Amsterdam, Netherlands: Elsevier (2006).

14. Atangana A, Baleanu D. New fractional derivatives with non-local and non-singular kernel: Theory and application to heat transfer model. *Therm Sci* (2016) 20:763–9. doi:10.2298/tsci160111018a

15. Pindza KMOE. Dynamics of fractional chaotic systems with Chebyshev spectral approximation method. *Int J Appl Comput Math* (2022) 8:140. doi:10.1007/s40819-022-01340-2

16. Avalos-Ruiz LF, Gomez-Aguilar JF, Atangana A, Owolabi KM. On the dynamics of fractional map with power-law, exponential decay and Mittag-Leffler memory. *Chaos, Solitons and Fractals* (2019) 127:364–88.

17. Owolabi KM, Atangana A. Computational study of multi-species fractional reaction-diffusion system with ABC operator. *Chaos Solitons Fractals* (2019) 128:280–9. doi:10.1016/j.chaos.2019.07.050

18. Alzabut J, Bolat Y, Abdeljawad T. Almost periodic dynamics of a discrete Nicholson's blowflies model involving a linear harvesting term. *Adv Differ Equ* (2012) 2012:158. doi:10.1186/1687-1847-2012-158

19. Alzabut J, Tyagi S, Abbas S. Discrete fractional-order BAM neural networks with leakage delay: Existence and stability results. *Asian J Control* (2020) 22:143–55. doi:10.1002/asjc.1918

20. Arfan M, Lashin MMA, Sunthrayuth P, Shah K, Ullah A, Iskakova K, et al. On nonlinear dynamics of COVID-19 disease model corresponding to nonsingular fractional order derivative. *Med Biol Eng Comput* (2022) 60:3169–85. doi:10.1007/s11517-022-02661-6

21. Cui M, Lin Y. *Nonlinear numerical analysis in the reproducing kernel space*. USA: Nova Science (2009).

22. Berlinet A, Agnan CT. *Reproducing kernel Hilbert space in probability and statistics*. USA: Kluwer Academic Publishers (2004).

23. Daniel A. *Reproducing kernel spaces and applications*. Switzerland: Springer (2003).

24. Abu Arqub O. The reproducing kernel algorithm for handling differential algebraic systems of ordinary differential equations. *Math Methods Appl Sci* (2016) 39:4549–62. doi:10.1002/mma.3884

25. Karaagac B, Owolabi KM, Nisar KS. Analysis and dynamics of illicit drug use described by fractional derivative with Mittag-Leffler kernel. *Comput Mater Contin* (2020) 65:1905–24. doi:10.32604/cmc.2020.011623

26. Jiang W, Chen Z. A collocation method based on reproducing kernel for a modified anomalous subdiffusion equation. *Numer Methods Partial Differ Equ* (2014) 30:289–300. doi:10.1002/num.21809

27. Geng FZ, Qian SP, Li S. A numerical method for singularly perturbed turning point problems with an interior layer. *J Comput Appl Math* (2014) 255:97–105. doi:10.1016/j.cam.2013.04.040

28. Lin Y, Cui M, Yang L. Representation of the exact solution for a kind of nonlinear partial differential equation. *Appl Math Lett* (2006) 19:808–13. doi:10.1016/j.aml.2005.10.010

29. Akgül A. A novel method for a fractional derivative with non-local and non-singular kernel. *Chaos Solitons Fractals* (2018) 114:478–82. doi:10.1016/j.chaos.2018.07.032

30. Ahmad S, Ullah A, Akgül A, Baleanu D. Analysis of the fractional tumour-immune-vitamins model with Mittag–Leffler kernel. *Results Phys* (2020) 19:103559. doi:10.1016/j.rinp.2020.103559

31. Siddique I, Akgül A. Analysis of MHD generalized first problem of Stokes' in view of local and non-local fractal fractional differential operators. *Chaos Solitons Fractals* (2020) 140:110161. doi:10.1016/j.chaos.2020.110161

32. Zhoua Y, Cui M, Lin Y. Numerical algorithm for parabolic problems with non-classical conditions. *J Comput Appl Math* (2009) 230:770–80. doi:10.1016/j.cam.2009.01.012